CHAPTER IV
PREPARATION AND CHARACTERIZATION OF MAGNESIUM-DOPED BARIUM STRONTIUM TITANATE VIA SOL-GEL METHOD

4.1 Abstract

High dielectric constant powders with various compositions of magnesium-doped barium strontium titanate, $Ba_{1-x-y}Sr_xMg_yTiO_3$ (where x = 0.3, 0.4, 0.5 and y = 0, 0.005, 0.010, 0.020) have been successfully prepared via sol-gel process at low temperature condition (60℃). The as-processed barium strontium titanate gel was characterized by TGA and DTA to determine the calcination temperature which ceramic phase was found to be fully crystallized at 900℃. The obtained magnesium-doped barium strontium titanate powder were characterized by XRD to confirm the phase formation of magnesium-doped barium strontium titanate. In addition, the measurement of frequency-dependent dielectric properties indicated that with increasing magnesium content, the dielectric constant decreases. Whereas, the temperature-dependent dielectric properties were slightly changed as a function of temperature.

4.2 Introduction

Barium titanate have been extensively well-known for past few decades in terms of producing capacitors, electrical transducers and ferroelectric random access memory (FeRAM), etc. due to its possession of very high permittivity and low loss at high frequency. According to its perovskite (ABO_3) structure, the structure of barium titanate can be changed in wide temperature range. One of the major problem of barium titanate is the fact that the tetragonal-cubic phase transition temperature or so-called Curie temperature, is very high (approximately 120℃). Many researches has been purposed in order to reduce phase transition temperature, dielectric constant and loss tangent by introducing the solid solution of $BaTiO_3$ and $SrTiO_3$, the effect of strontium substitution are reduction of ferroelectric transition temperature,

suppression of dielectric and loss tangent for high and low frequency range, and reduction of unit cell volume [1]. Another idea to suppress dielectric constant and loss tangent is to dope magnesium dopant in barium strontium titanate [2]. These two concept not only can improve the Curie temperature, but they also suppress dielectric permittivity, loss tangent and lattice parameters. Moreover, they are applicable in microwave tunable applications. The barium titanate and its solid solutions have been mostly prepared from traditional solid state reaction. Thereafter, sol-gel processes has been used to produce the powder, accordingly, their easiness to control the composition, low-temperature combination and delicate particle size [3].

In this work, we prepared the magnesium-doped barium strontium titanate powder by using low temperature sol-gel process. By varying the mole ratios of strontium substituents and magnesium dopant. Twelve composition of magnesium-doped barium strontium titanate, $Ba_{1-x-y}Sr_xMg_yTiO_3$ (where x = 0.3, 0.4, 0.5 and y = 0, 0.005, 0.010, 0.020), have been prepared to study the effect of strontium substituents and magnesium dopant on the phase formation, frequency-dependent and temperature-dependent dielectric properties.

4.3 Experimental

4.3.1 Preparation of Magnesium-doped Barium Strontium Titanate Powder

The gel products of magnesium-doped barium strontium titanate, $Ba_{1-x-y}Sr_xMg_yTiO_3$ (where x = 0.3, 0.4, 0.5 and y = 0, 0.005, 0.010, 0.020) were prepared as follows. Firstly, stoichiometric ratios of barium acetate, strontium acetate varying mole fraction x = 0.3, 0.4, 0.5 and magnesium acetate dopant varying mole fraction y = 0, 0.005, 0.010, 0.020 were dissolved in 50 ml of glacial acetic acid and stirred at 60 ℃ for 15 min. Then, 50 ml of methanol was added to the mixture and stirred for 15 min. Then, titanium-n-butoxide solution was added to the mixture. The overall mole ratio of barium ions, strontium ions, magnesium ions and titanium ions are shown in Table 4.1. Subsequently, the homogeneously mixed precursor solution was stirred for 20 h until the solution became the white gel. Finally, the obtained gels were further taken to calcination process by using "2-step

decomposition" method to obtain white powder products, the temperature profile of this method is shown in Figure 4.1.

Table 4.1 The overall mole ratio of barium ions, strontium ions, magnesium ions and titanium ions

$Ba_{1-x-y}Sr_xMg_yTiO_3$		Molar ratio			
x	y	Ba	Sr	Mg	Ti
0.3	0	0.7	0.3	0	1
	0.005	0.695		0.005	0.995
	0.01	0.69		0.01	0.99
	0.02	0.68		0.02	0.98
0.4	0	0.6	0.4	0	1
	0.005	0.595		0.005	0.995
	0.01	0.59		0.01	0.99
	0.02	0.58		0.02	0.98
0.5	0	0.5	0.5	0	1
	0.005	0.495		0.005	0.995
	0.01	0.49		0.01	0.99
	0.02	0.48		0.02	0.98

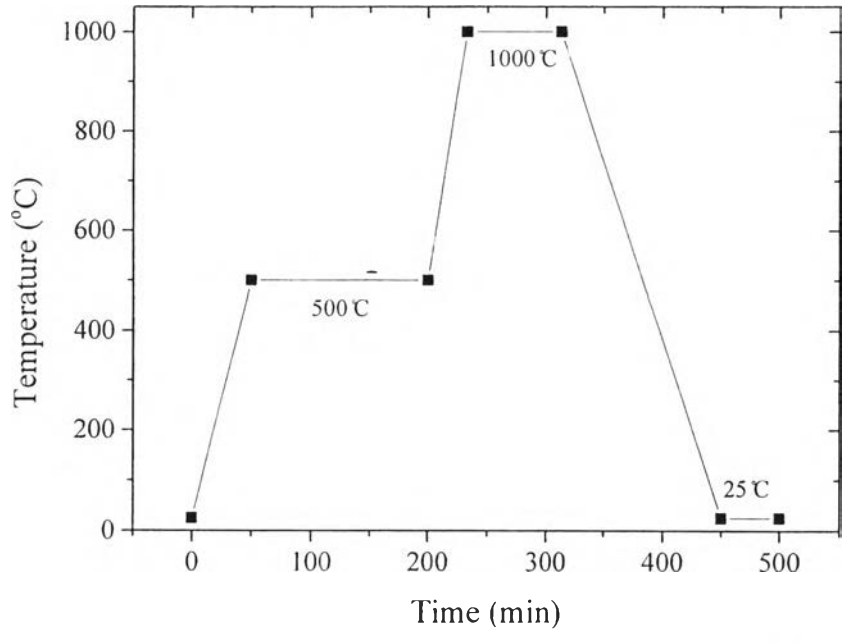

Figure 4.1 The temperature profile of 2-step decomposition method.

4.3.2 Characterizations and Testing

The Fourier transform infrared spectroscopy (FT-IR) was used to confirm the functional groups related to structure of barium acetate, strontium acetate, magnesium acetate and titanium-n-butoxide precursors, as well as the molecular structure of barium strontium titanate gel and powder. The FTIR spectra were obtained in a spectral range of 4000-800 cm^{-1} as a function of time with 64 scans at a resolution of 2 cm^{-1}. Thermal properties during calcination process of barium strontium titanate gel were measured by using Thermogravimetric Analysis (TGA) and Differential thermal analysis (DTA) techniques. The gel sample was heated from room temperature to 1,100℃ in air by using a heating rate of 10℃/min. The phase formations of magnesium-doped barium strontium titanate powders were characterized by X-ray diffractometer with Ni-filter CuKα radiation operated at 40 kV and 30 mA with scan speed 5 degree/min. The 2-theta was ranging from 20.00 degree to 80.00 degree. The obtained powder after calcination process were ground and hydraulic pressed inside uniaxial pressing mold and two side of compacted powder specimens were electroded with silver paint. Dielectric properties [dielectric

constant (ε'), and loss tangent (tan δ ; ε"/ε')] of magnesium-doped barium strontium titanate specimens were determined by using an E4991A RF impedance/material analyzer equipped with a 16453A dielectric material test fixture, Agilent Technologies, Inc., USA). The frequency-dependent dielectric properties were measured by using scan frequencies ranged from 1 MHz to 1 GHz. To study the temperature-dependent dielectric properties, the compact powder specimens were placed between two electrodes inside an Espec SU-261 temperature and humidity control chamber, the specimens were heated from room temperature to 150℃ and then cooled down by 10℃ each time. The data were collected every 5 min after temperature is decreased.

4.4 Results and Discussion

4.4.1 Barium Strontium Titanate Precursors and Gel Characterizations

4.4.1.1 Fourier Transform Infrared Spectroscopy (FTIR) Analysis

The FTIR spectra of starting precursors and the as-processed gel were shown in Figure 4.2(a) - 4.2(e). In Figure 4.2(a) to 4.2(c) show the similar spectra of acetate group of precursors due to the present of hydroxyl –OH stretching band at approximately 3400 cm^{-1} and carboxylate stretching band appeared at 1600 cm^{-1}. When the precursors solution became a gel, there were three distinguished peaks in barium strontium titanate gel FTIR spectrum as shown in Figure 4.2(e) which were the hydroxyl -OH stretching band appeared at 3500 cm^{-1}, the carboxylate C=O stretching band appeared at 1600 cm^{-1} and the CH_2-CO bending vibration or -COOH coupled with -OH bending and C-O stretching vibration bands appeared at 1420 cm^{-1} [4].

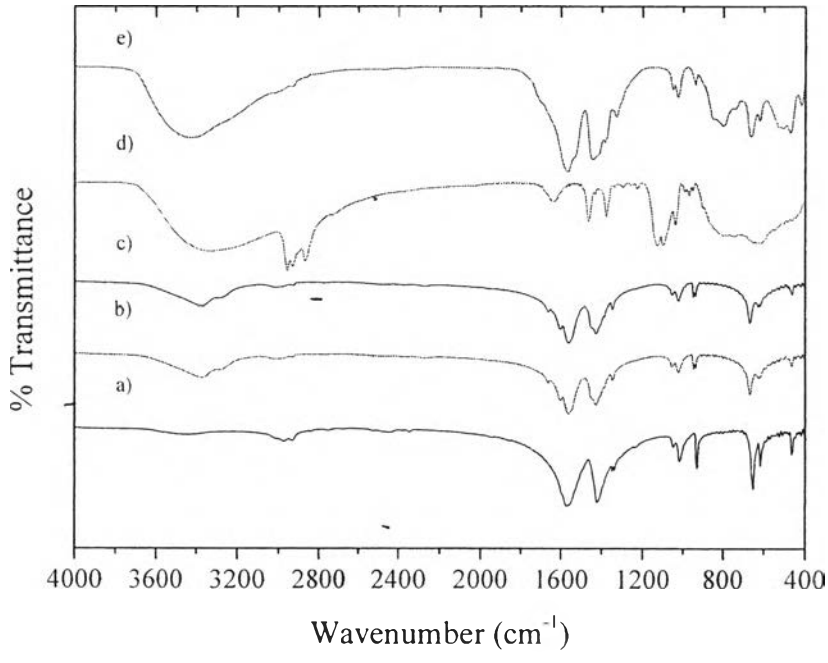

Figure 4.2 FTIR-spectra of (a) Barium acetate (b) Strontium acetate (c) Magnesium acetate (d) Titanium-n-butoxide and (e) Barium strontium titanate gel.

4.4.1.2 Differential Thermal Analysis (DTA) and Thermogravimetric Analysis (TGA)

While the as-processed gel was subjected to the heat from ambient temperature to 1,100℃ during TGA and DTA analysis as shown in Figure 4.3 and 4.4, respectively. In Figure 4.4, the first endothermic peak of DTA plot between 100℃ and 150℃ exhibit the water vaporization [5], which is correlated to weight loss around 71.74% in TGA thermogram as shown in Figure 4.3. The second endothermic peak of DTA between 300℃ and 400℃ demonstrates the dissociation of acetate group corresponding to 9.42% weight loss in TGA thermogram. Finally, the exothermic peak between 600℃ and 900℃ in DTA thermogram indicated the crystallization of barium strontium titanate ceramic phase. During the calcination process, the phase evolution began at 600℃ and became sharper at the temperature upper than 800℃ [6]. In addition, from TGA and DTA results, the calcined temperature for the obtained gel was found to be fully crystallized at 900℃ and the powder product yield obtained was found to be 18.84% of total gel weight.

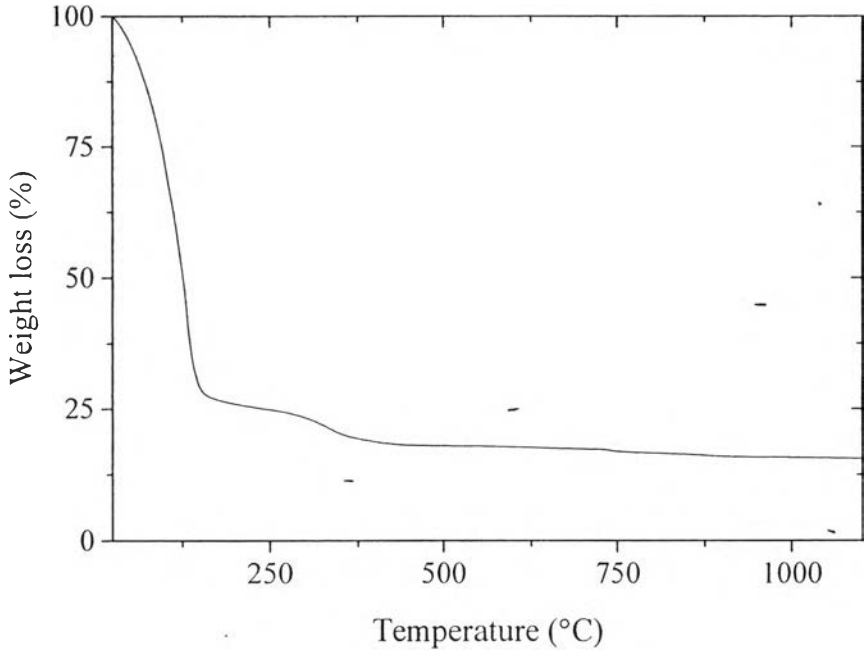

Figure 4.3 TGA thermogram of barium strontium titanate, $Ba_{0.7}Sr_{0.3}TiO_3$ gel.

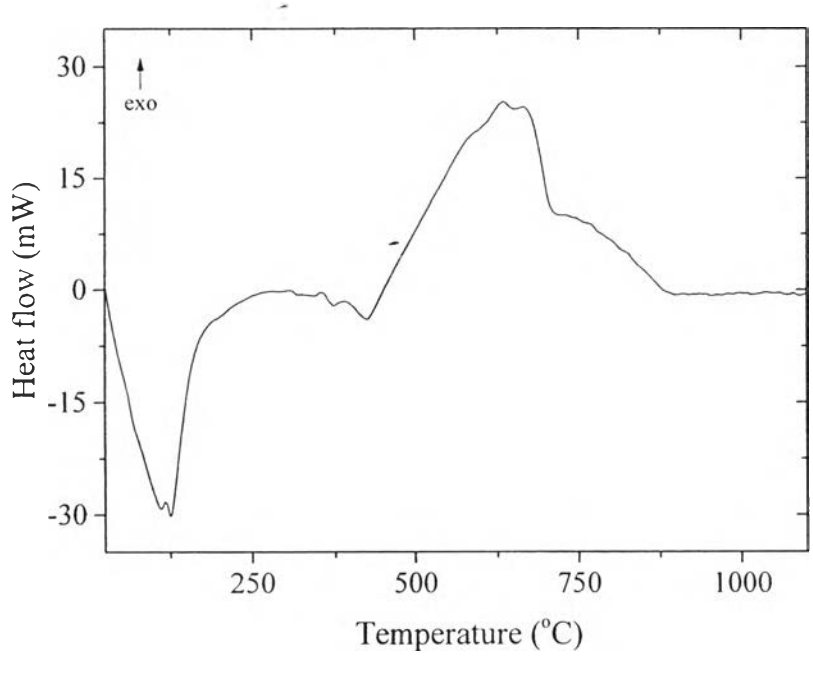

Figure 4.4 DTA thermogram of barium strontium titanate, $Ba_{0.7}Sr_{0.3}TiO_3$ gel.

4.4.2 Magnesium-doped Barium Strontium Titanate Gel and Powder Characterizations

4.4.2.1 Fourier Transform Infrared Spectroscopy (FTIR) Analysis

The FTIR spectrum of barium strontium titanate as-processed gel was shown in Figure 4.5. The O-H stretching band was represented around 3400 cm^{-1}, the band of CH_2-CO- bending vibration or –COOH coupled with O-H bending and C-O stretching vibration bands at ~1400 and ~1500 cm^{-1} [4] which became weaken down in the intensity after calcination process. In other words, the organic compounds in the barium strontium titanate gel have been disintegrated during the calcination process and finally became barium strontium titanate powder. As shown in Figure 4.6, FTIR spectrum of barium strontium titanate powder calcined at 900℃ showed two compelling peaks of the symmetrical vibrations and bending vibrations (in plane) of COO- group at 1430 cm^{-1} and 850 cm^{-1}, respectively [7].

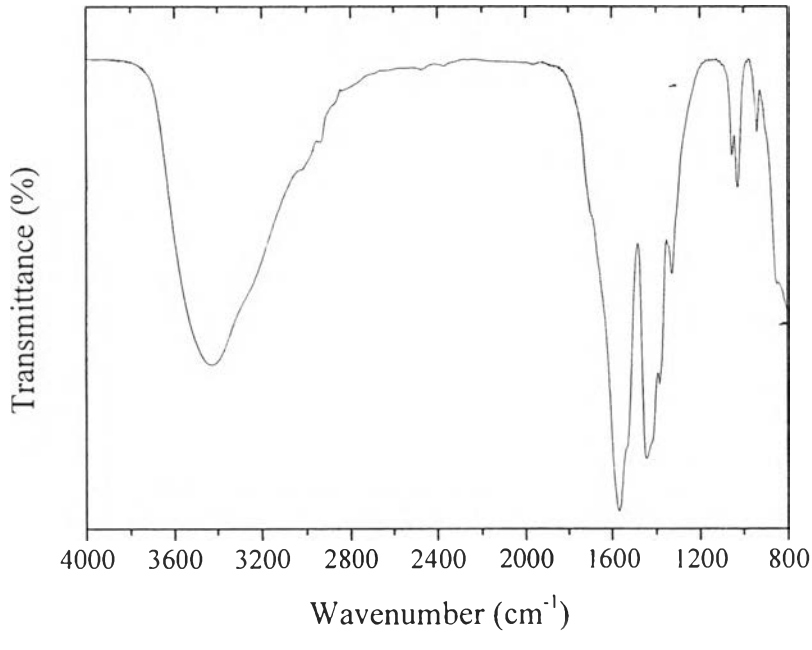

Figure 4.5 FTIR-spectrum of barium strontium titanate gel.

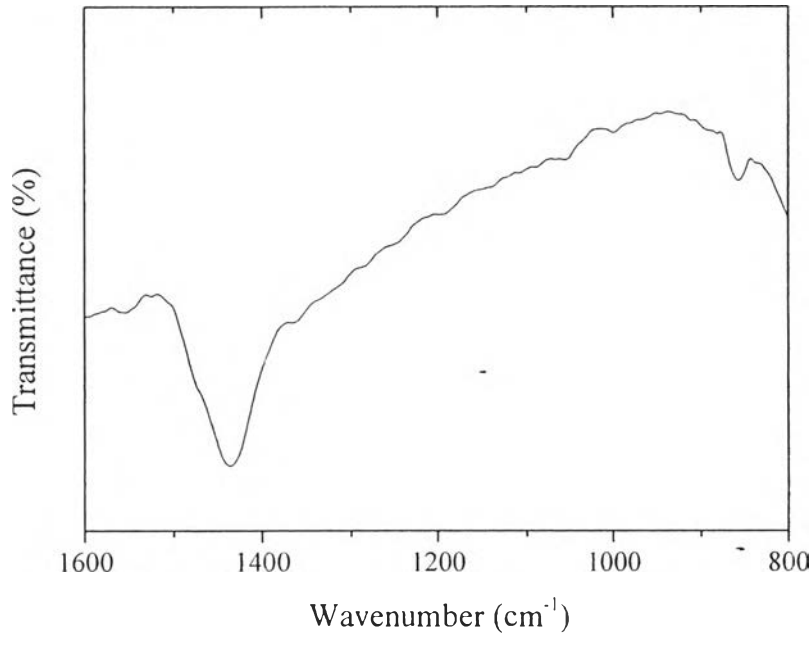

Figure 4.6 FTIR-spectrum of barium strontium titanate powder.

4.4.2.2 Morphological Investigation and Particle Size Analysis

The calcined powder was investigated on the morphology as shown in Figure 4.7. The SEM image show the rounded-square and circular shape of the particle. The size were ranging between 100 nm to 250 nm. Whereas, the particle size were double checked by using particle size analyzer. The result show the mean size distribution of particle was about 300 nm in diameter.

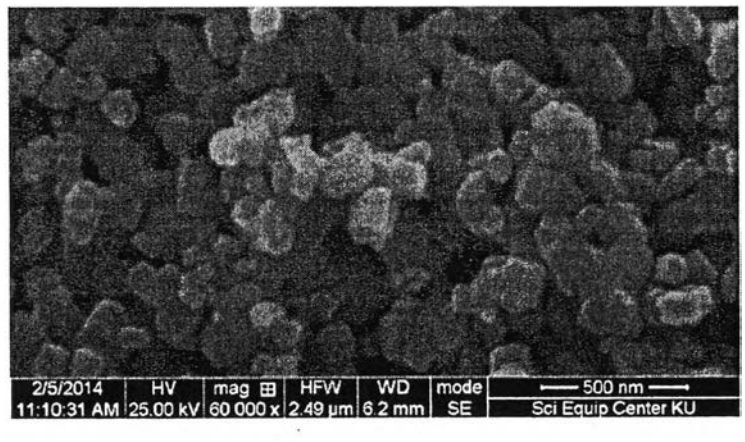

Figure 4.7 SEM image of barium strontium titanate powder.

4.4.2.3 X-Ray Diffraction (XRD) Phase Analysis

The X-Ray diffraction patterns in Figure 4.8, which reveals the transformation from barium strontium titanate gel which have amorphous phase (Figure 4.8(a)) to powder which have crystalline phase (Figure 4.8(b)) and the possession of tetragonal perovskite structure of $Ba_{0.7}Sr_{0.3}TiO_3$ powder. According to JCPD PDF card number 89-0279, the perovskite structure exhibit 100, 110, 111, 200, 201, 211, 220, 212, and 310 planes in 2theta Bragg Angle 22.510, 31.932, 39.351, 45.789, 51.529, 56.868, 66.628, 71.326, and 75.749 degree respectively.

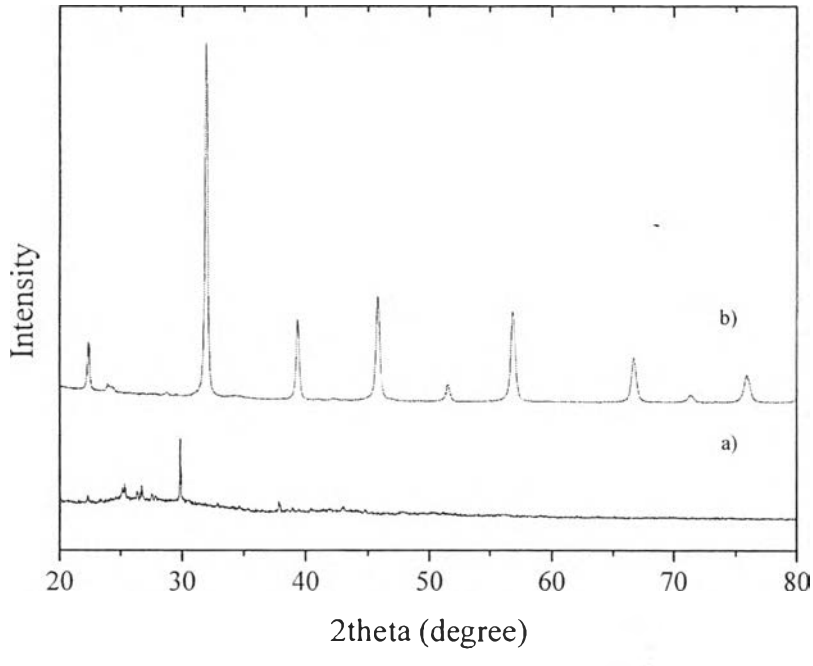

Figure 4.8 The X-Ray diffraction patterns of (a) barium strontium titanate gel and (b) barium strontium titanate powder.

The X-Ray diffraction patterns in Figure 4.9 to Figure 4.11 exhibit the peaks of magnesium-doped barium strontium titanate which have the same peaks as the pattern shown in Figure 4.8. However, the XRD patterns did not show any distinct planes of the secondary phases such as titanium-rich phase ($Ba_4Ti_{16}O_3$) [5] or magnesium oxide (MgO) [6].

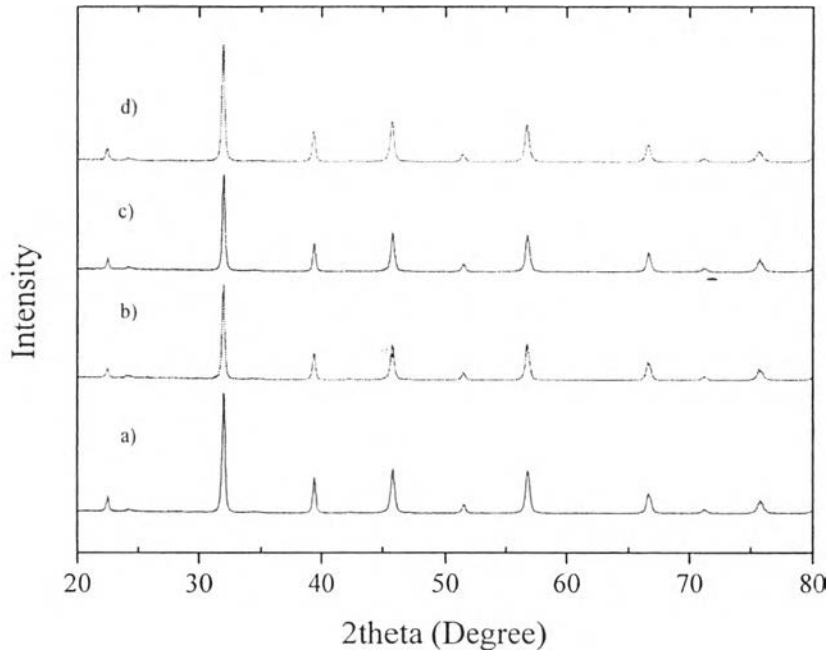

Figure 4.9 XRD patterns of $Ba_{1-x-y}Sr_xMg_yTiO_3$ powder (where x = 0.3 and y = (a) 0, (b) 0.005, (c) 0.010, (d) 0.020).

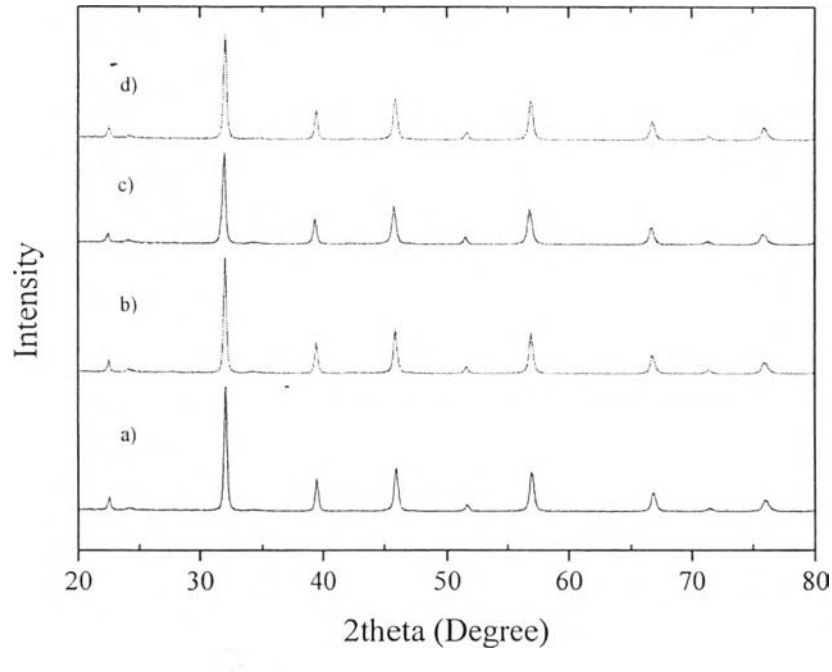

Figure 4.10 XRD patterns of $Ba_{1-x-y}Sr_xMg_yTiO_3$ powder (where x = 0.4 and y = (a) 0, (b) 0.005, (c) 0.010, (d) 0.020).

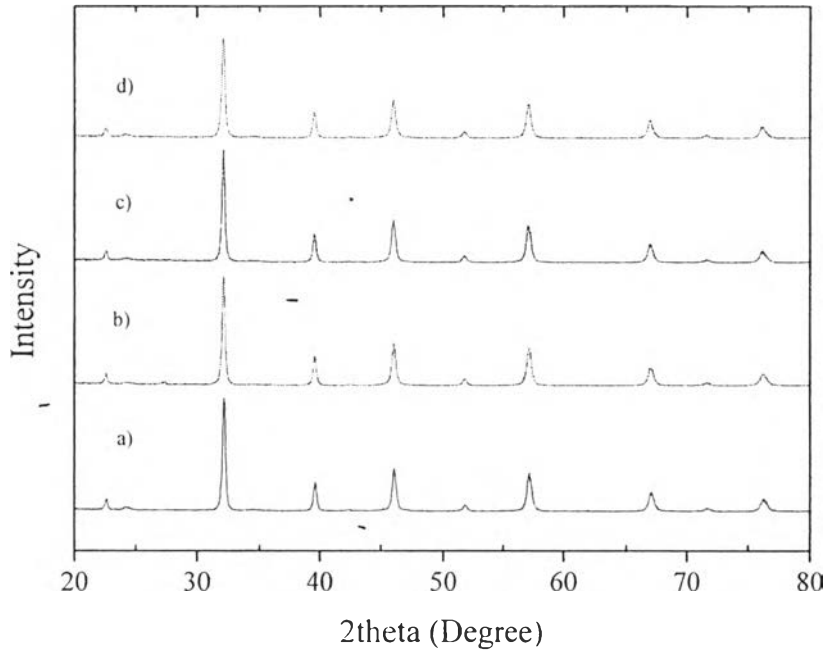

Figure 4.11 XRD patterns of $Ba_{1-x-y}Sr_xMg_yTiO_3$ powder (where x = 0.5 and y = (a) 0, (b) 0.005, (c) 0.010, (d) 0.020).

Therefore, in order to study the effects of magnesium dopant in the barium strontium titanate compounds, the composition of Ba^{2+}, Sr^{2+}, Mg^{2+}, and Ti^{4+} were then investigated by using x-ray fluorescence technique and the lattice parameters of magnesium-doped barium strontium titanate powder were also calculated in the tetragonal form from the equation:

$$\frac{1}{d^2} = \frac{h^2 + k^2}{a^2} + \frac{l^2}{c^2} \qquad (4.1)$$

where *d* is distance between planes from the Miller index (h k l) and the unit cell dimensions a,b,c

Table 4.2 Lattice parameters of $Ba_{1-x-y}Sr_xMg_yTiO_3$ powder and quantitative analysis of Ba^{2+}, Sr^{2+}, Mg^{2+}, and Ti^{4+}

$Ba_{1-x-y}Sr_xMg_yTiO_3$		Actual composition (%)				Lattice Parameter		
x	y	Ba	Sr	Mg	Ti	a	c	c/a
0.3	0	52.75	19.63	-	27.60	3.9514	4.0339	1.0209
	0.005	58.01	15.08	0.08	26.83	3.9573	4.0212	1.0161
	0.01	56.71	15.67	0.12	27.48	3.9556	4.0242	1.0173
	0.02	56.36	13.38	0.26	29.99	3.9626	4.0144	1.0131
0.4	0	49.87	20.68	-	29.44	3.9468	3.9969	1.0127
	0.005	54.29	19.69	0.08	25.94	3.9514	3.9957	1.0112
	0.01	53.19	18.46	0.12	28.22	3.9573	3.9997	1.0107
	0.02	50.32	18.66	0.22	30.80	3.9500	3.9944	1.0112
0.5	0	60.67	14.10	-	25.23	3.9329	3.9958	1.0160
	0.005	47.73	23.10	0.05	29.10	3.9366	3.9912	1.0139
	0.01	50.46	23.95	0.15	25.44	3.9391	3.9978	1.0149
	0.02	50.78	23.03	0.21	25.97	3.9435	3.9756	1.0081

Table 4.2 present the lattice parameter of $Ba_{1-x-y}Sr_xMg_yTiO_3$ powder and oxide compound quantitative analysis of Ba^{2+}, Sr^{2+}, Mg^{2+}, and Ti^{4+} content contained in $Ba_{1-x-y}Sr_xMg_yTiO_3$ powder. The result indicated that, with increasing amount of magnesium dopants in barium strontium titanate compounds, the quantity of Mg^{2+} increases. In other word, the magnesium dopants were somewhat loaded into the barium strontium titanate powder. Furthermore, the increasing amount of strontium and magnesium loading affected in the reduction of lattice parameter such as a, c and tetragonality (c/a ratio). It is due to the fact that, the strontium ions and magnesium ions have lower atomic radii than those of barium ions. The substitution of strontium ion took place at the barium site (A-site substitution in ABO_3 Perovskite structure) [1]. As well as magnesium dopant, the Mg^{2+} can occupy either at Ba^{2+} site or Sr^{2+} site [8]. In both cases, the lattice parameter tends to decrease with increasing amount of substituents.

4.4.2.4 Crystallite Size Analysis

The crystallites size (D) values calculated by using Scherrer's equation from 110 plane in XRD data are shown in Table 4.3. The crystallite of magnesium-doped barium strontium titanate, $Ba_{1-x-y}Sr_xMg_yTiO_3$ (where x = 0.3, 0.4, 0.5 and y = 0, 0.005, 0.010, 0.020) were varied from 29 nm to 42 nm. Which are smaller than those of particle size. It can be argued that magnesium-doped barium strontium titanate particles consist of polycrystalline phases.

Scherrer equation:

$$D_p = \frac{0.94\lambda}{\beta_{1/2}cos\theta} \qquad (4.2)$$

where D_p is Average crystallite size, β is line broadening in radians (FWHM), θ is Bragg angle and λ is X-ray wavelength.

Table 4.3 Crystallite size magnesium-doped barium strontium titanate particles calculated on 110 plane

$Ba_{1-x-y}Sr_xMg_yTiO_3$		Measured on 110 plane			
x	y	2-Theta	d(A)	FWHM	Crystallize size (nm)
0.3	0	31.9470	2.7990	0.2470	34.9571
	0.005	31.9070	2.8024	0.2180	39.6034
	0.01	31.9200	2.8013	0.2060	41.9118
	0.02	31.8770	2.8051	0.2480	34.8101
0.4	0	32.0120	2.7935	0.2370	36.4380
	0.005	31.9830	2.7960	0.2330	37.0609
	0.01	31.9220	2.8012	0.2960	29.1685
	0.02	31.9890	2.7955	0.2630	32.8339
0.5	0	32.1230	2.7841	0.2600	33.2239
	0.005	32.0940	2.7866	0.2510	34.4127
	0.01	32.0710	2.7886	0.2580	33.4771
	0.02	32.0600	2.7894	0.2810	30.7361

4.4.2.5 Frequency-dependent Dielectric Properties Measurements

From Figure 4.12, 4.13, and 4.14 show frequency-dependent dielectric constant of magnesium-doped barium strontium titanate powder, $Ba_{1-x-y}Sr_xMg_yTiO_3$ at the frequency ranging from 1 MHz to 100 MHz. The results show the remarkable value of dielectric constant of $Ba_{1-x-y}Sr_xMg_yTiO_3$, which gives the highest dielectric constant at the composition when strontium content of 30 mol% and magnesium content of 0 mol% or $Ba_{0.7}Sr_{0.3}TiO_3$. The dielectric constant of $Ba_{1-x-y}Sr_xMg_yTiO_3$ powder was decreased respectively with increasing amount of strontium and magnesium content. And the lowest value of dielectric constant belongs to the composition of strontium content of 50 mol% and magnesium content is 2 mol% or $Ba_{0.5}Sr_{0.5}Mg_{0.02}TiO_3$.

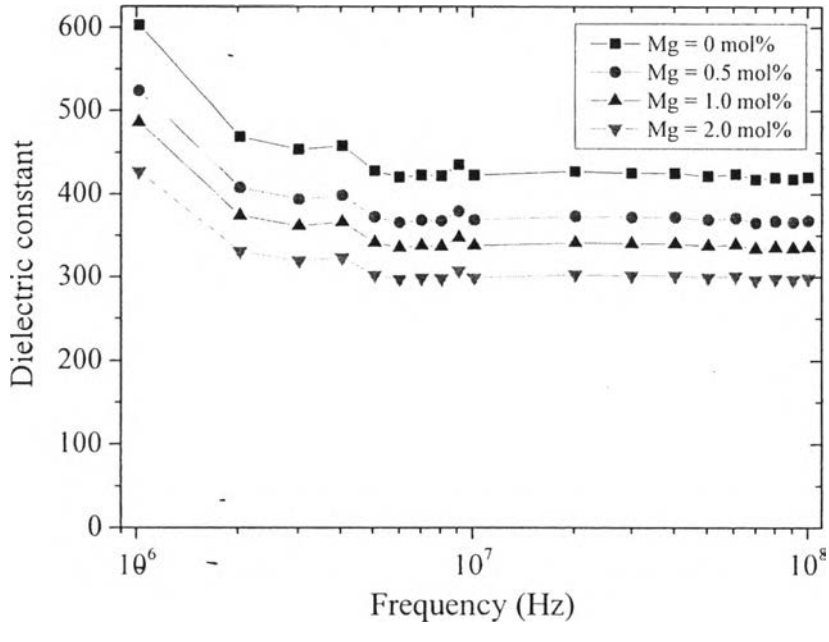

Figure 4.12 Frequency-dependent dielectric constant of $Ba_{1-x-y}Sr_xMg_yTiO_3$ powder (where x = 0.3 and y = 0, 0.005, 0.010, 0.020).

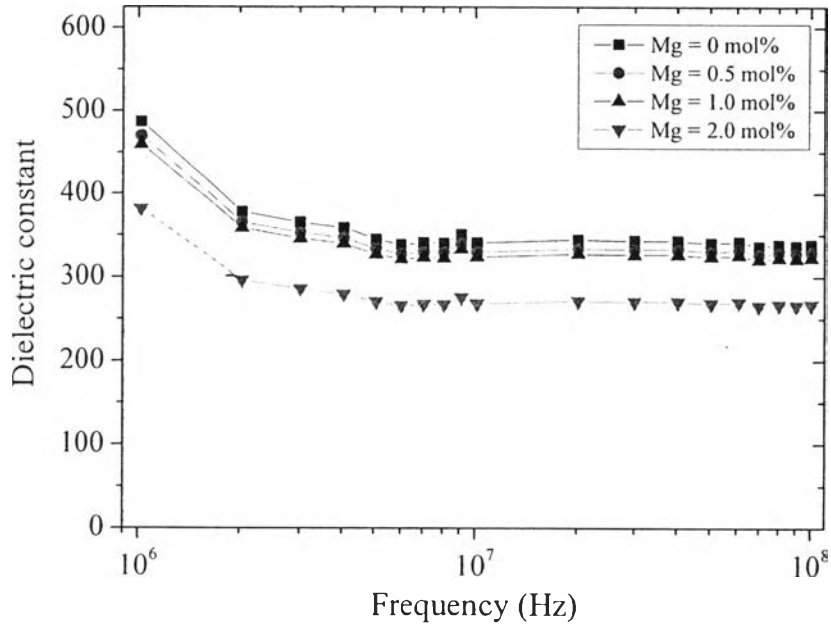

Figure 4.13 Frequency-dependent dielectric constant of $Ba_{1-x-y}Sr_xMg_yTiO_3$ powder (where x = 0.4 and y = 0, 0.005, 0.010, 0.020).

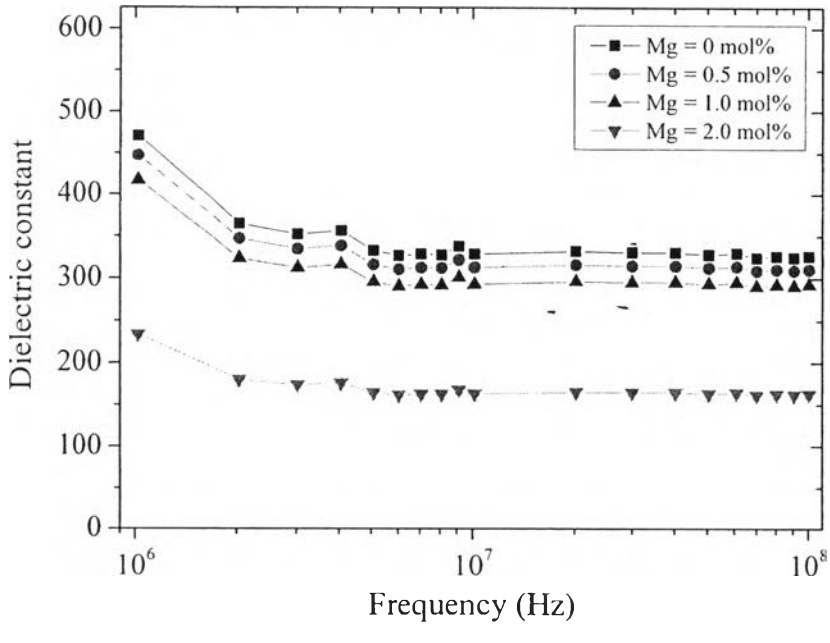

Figure 4.14 Frequency-dependent dielectric constant of $Ba_{1-x-y}Sr_xMg_yTiO_3$ powder (where x = 0.5 and y = 0, 0.005, 0.010, 0.020).

The loss tangent of magnesium-doped barium strontium titanate powders in Figure 4.15, 4.16, and 4.17, however, appeared to be remained stable as the function of frequency. The slightly reduction of loss tangent was a function of magnesium content. Therefore, the loss tangent values of magnesium-doped barium strontium titanate powders showed very low values and the loss tangent were not exceed over 0.03. In other word, there were only small amount of electrical energy has been dissipated during applying the electric field.

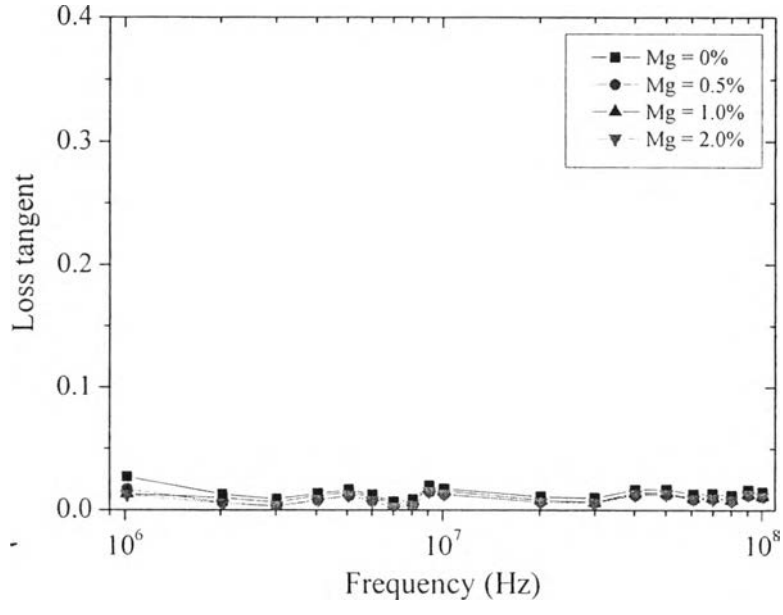

Figure 4.15 Frequency-dependent loss tangent of $Ba_{1-x-y}Sr_xMg_yTiO_3$ powder (where x = 0.3 and y = 0, 0.005, 0.010, 0.020).

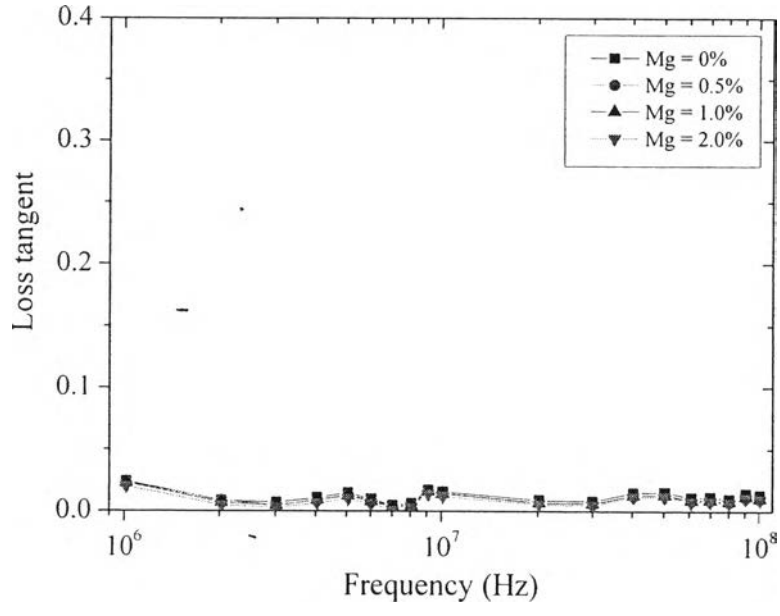

Figure 4.16 Frequency-dependent loss tangent of $Ba_{1-x-y}Sr_xMg_yTiO_3$ powder (where x = 0.4 and y = 0, 0.005, 0.010, 0.020).

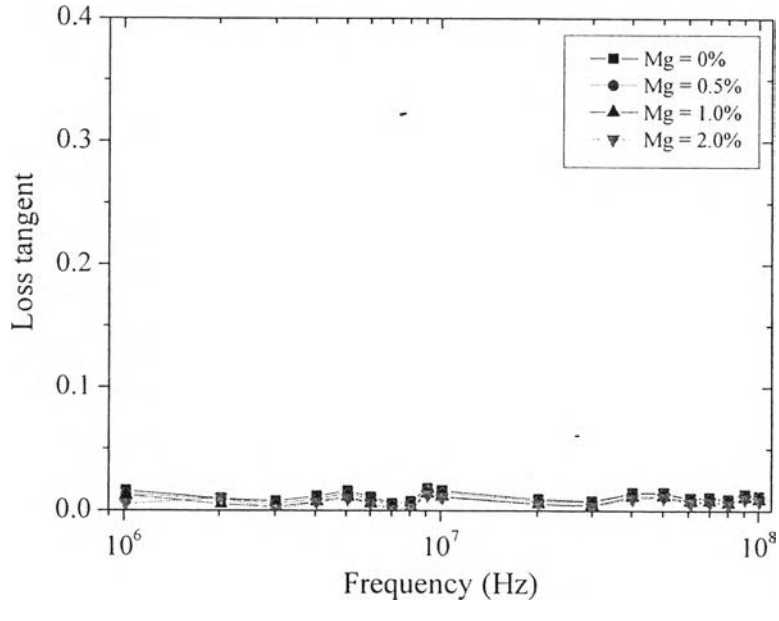

Figure 4.17 Frequency-dependent loss tangent of $Ba_{1-x-y}Sr_xMg_yTiO_3$ powder (where x = 0.5 and y = 0, 0.005, 0.010, 0.020).

4.4.2.6 Temperature-dependent Dielectric Properties Measurements

The temperature-dependent dielectric properties of magnesium-doped barium strontium titanate (Figure 4.18, 4.19, and 4.20) measured from 20℃ to 150℃ at 10 MHz. The dielectric constant of magnesium-doped barium strontium titanate were slightly decreases as a function of temperature and the phase transition peaks were not appeared in these temperature range.

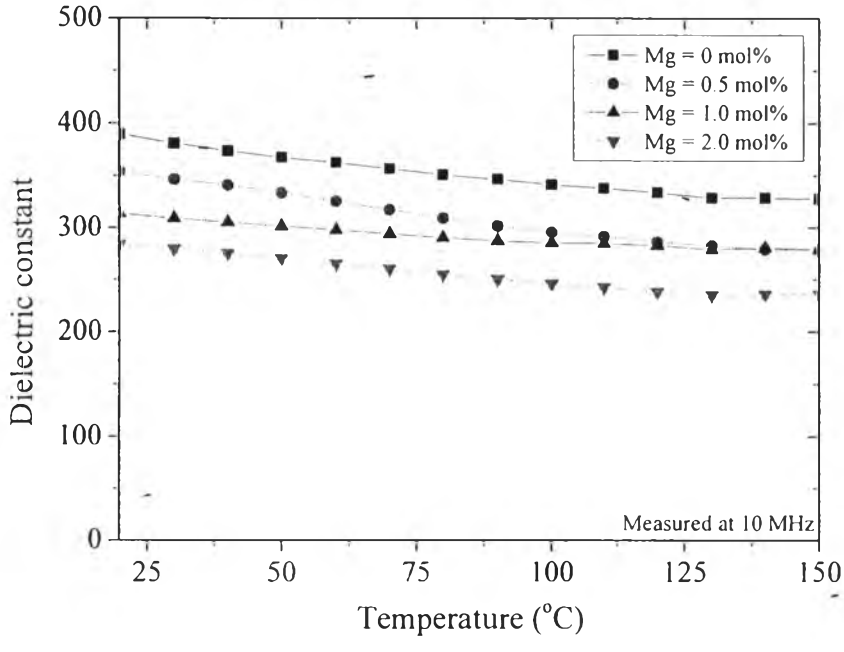

Figure 4.18 Temperature-dependent dielectric constant of $Ba_{1-x-y}Sr_xMg_yTiO_3$ powder (where x = 0.3 and y = 0, 0.005, 0.010, 0.020).

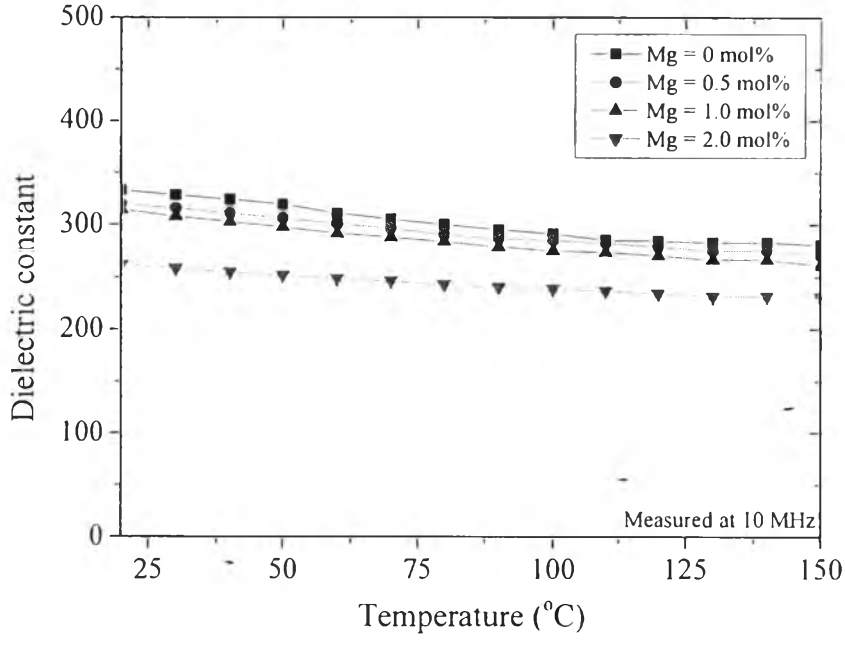

Figure 4.19 Temperature-dependent dielectric constant of $Ba_{1-x-y}Sr_xMg_yTiO_3$ powder (where x = 0.4 and y = 0, 0.005, 0.010, 0.020).

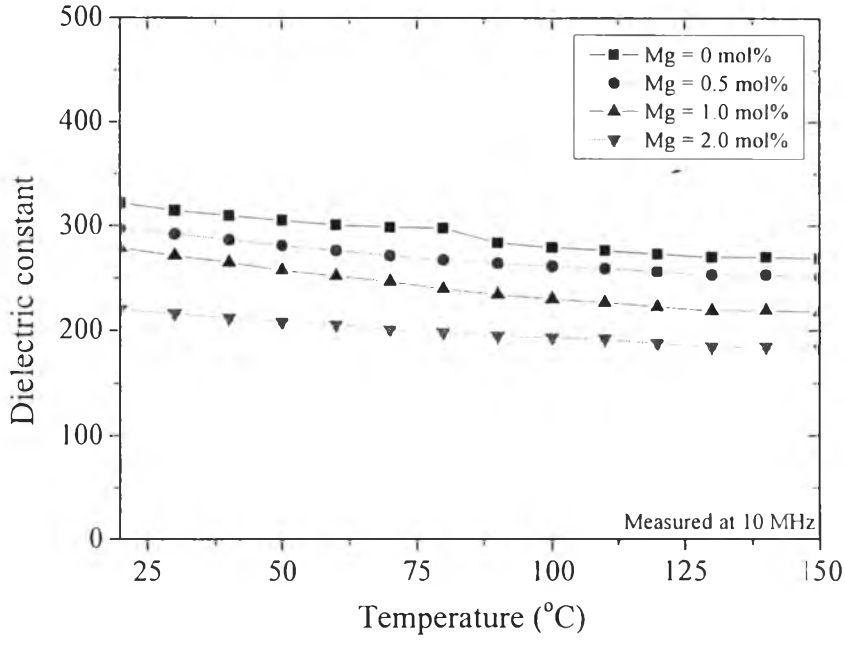

Figure 4.20 Temperature-dependent dielectric constant of $Ba_{1-x-y}Sr_xMg_yTiO_3$ powder (where x = 0.5 and y = 0, 0.005, 0.010, 0.020).

On the other hand, the loss tangent of magnesium-doped barium strontium titanate (as shown in Figure 4.21, 4.22, and 4.23) has slightly raised from 20℃ toward 150℃, which could be implicated to thermal activated conductivity [9] and lowering down the dielectric constant.

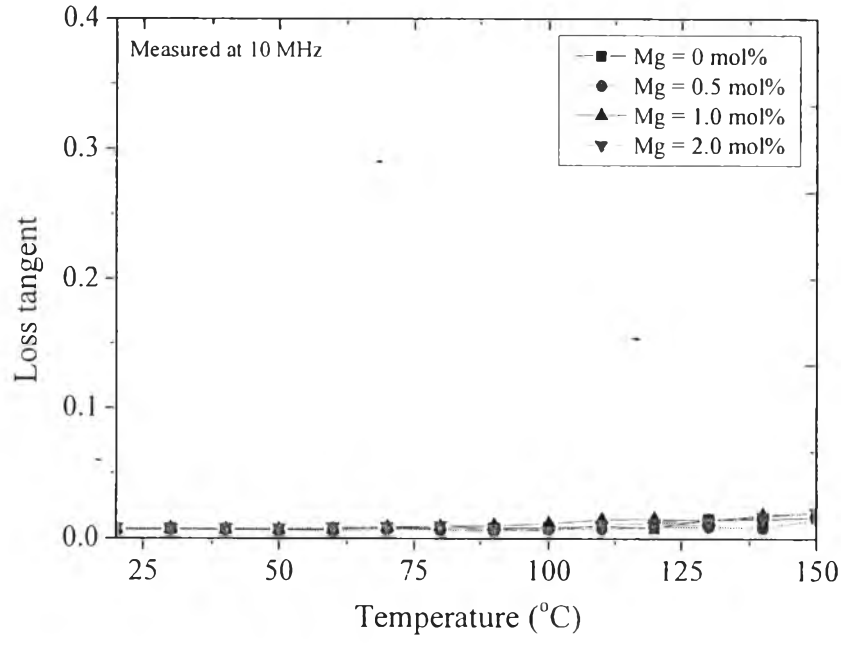

Figure 4.21 Temperature-dependent loss tangent of $Ba_{1-x-y}Sr_xMg_yTiO_3$ powder (where x = 0.3 and y = 0, 0.005, 0.010, 0.020).

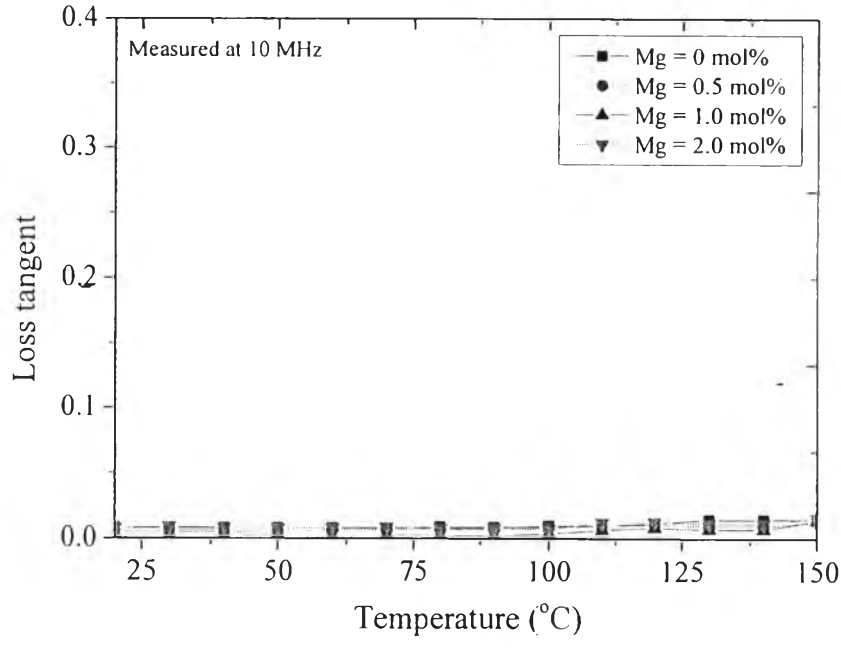

Figure 4.22 Temperature-dependent loss tangent of $Ba_{1-x-y}Sr_xMg_yTiO_3$ powder (where x = 0.5 and y = 0, 0.005, 0.010, 0.020).

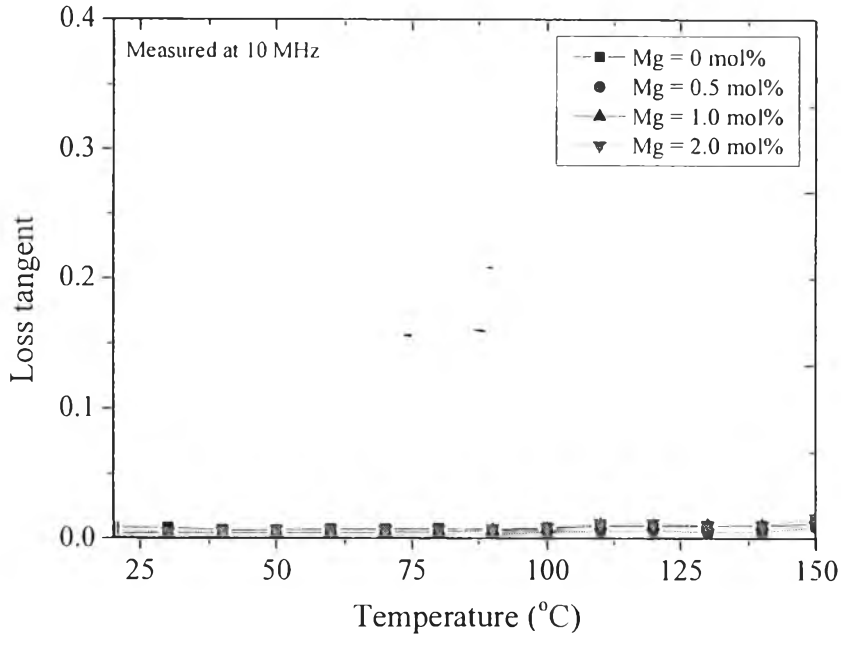

Figure 4.23 Temperature-dependent loss tangent of $Ba_{1-x-y}Sr_xMg_yTiO_3$ powder (where x = 0.5 and y = 0, 0.005, 0.010, 0.020).

4.4.2.7 The Relationship Between Lattice Parameter and Dielectric Constant of $Ba_{1-x-y}Sr_xMg_yTiO_3$ Powder

The relationship between dielectric constant and lattice parameter of $Ba_{1-x-y}Sr_xMg_yTiO_3$ powder (which x = 0.3, 0.4, 0.5 and y = 0, 0.005, 0.010, 0.020) are shown in Figure 4.24, 4.25, and 4.26. As a result of increasing amount of magnesium-dopant in single amount of strontium content, the tetragonality (c/a ratio) have tendency to decrease and move closer to 1 or the structure of magnesium-doped barium strontium titanate unit cell has been transformed from tetragonal to cubic phase (or pseudo cubic). Which influence the polarization in the unit cell were generated in smaller amount and cause the dielectric constant to be reduced as the magnesium content increase due to the smaller amount of polarizations were generated. Whereas, the increasing amount of magnesium ions were beneficial in suppressing loss tangent.

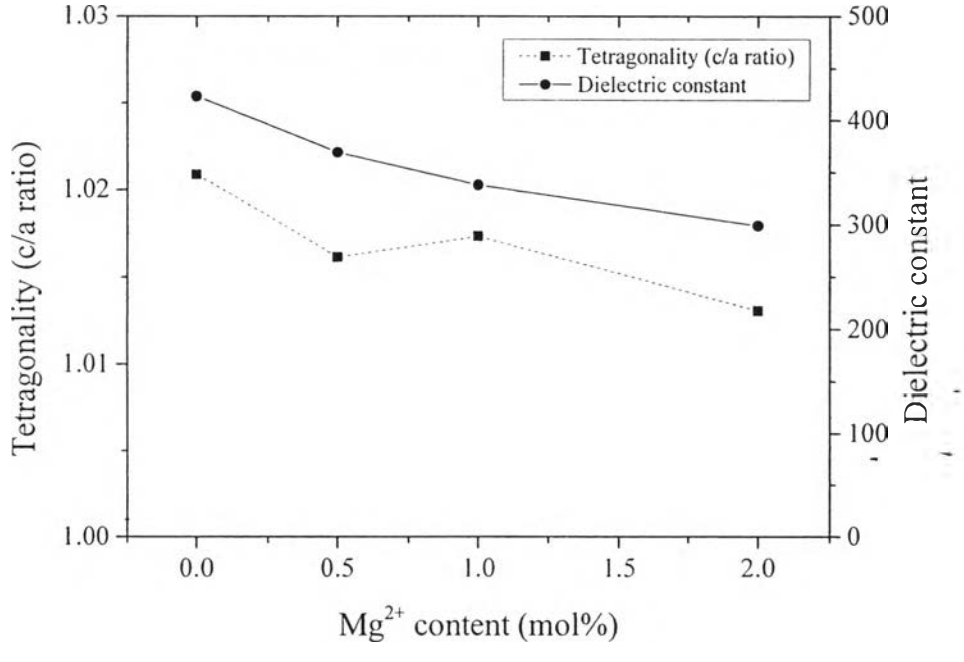

Figure 4.24 Dielectric constant and lattice parameter relationship of $Ba_{1-x-y}Sr_xMg_yTiO_3$ powder (which x = 0.3 and y = 0, 0.5, 1.0, 2.0).

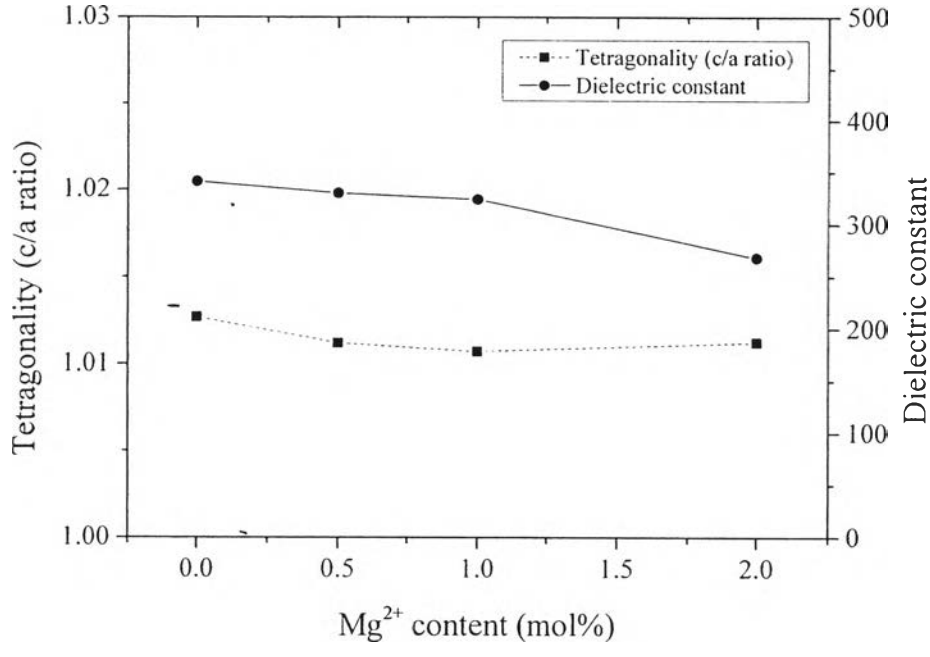

Figure 4.25 Dielectric constant and lattice parameter relationship of $Ba_{1-x-y}Sr_xMg_yTiO_3$ powder (which x = 0.4 and y = 0, 0.5, 1.0, 2.0).

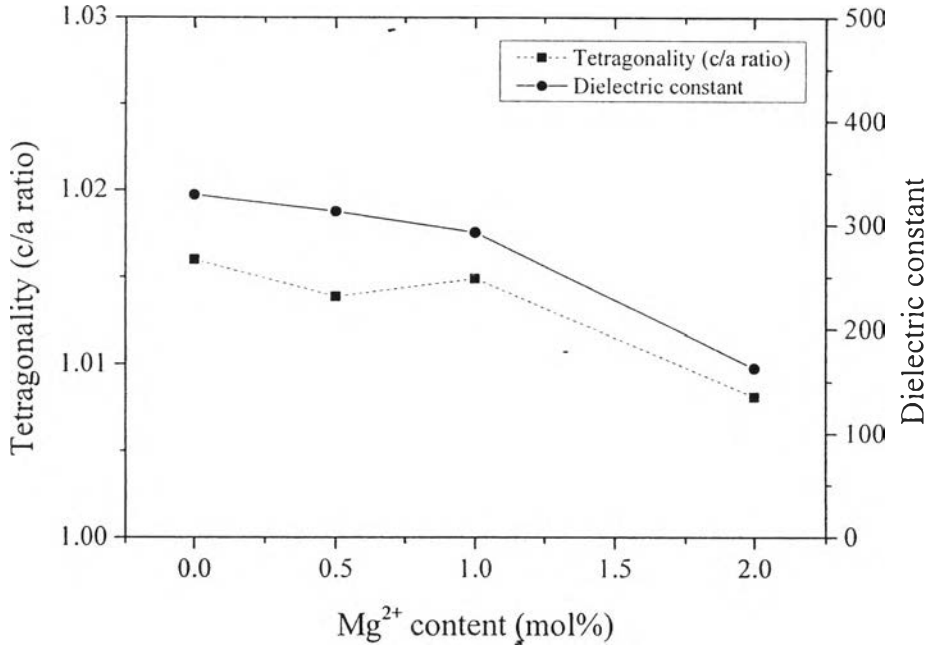

Figure 4.26 Dielectric constant and lattice parameter relationship of $Ba_{1-x-y}Sr_xMg_yTiO_3$ powder (which x = 0.5 and y = 0, 0.5, 1.0, 2.0).

4.5 Conclusions

We have successfully synthesized magnesium-doped barium strontium titanate nanoparticles by low-temperature (60℃) sol-gel process. The powder phases were fully-crystallized from gel after calcinating at 900℃. The obtained powders from calcination process showed the dielectric properties depending on the content of magnesium as shown in Table 4.4. Moreover, the frequency-dependent and temperature-dependent dielectric properties were functions of strontium and magnesium content. However, the loss tangents of magnesium-doped barium strontium titanate were not exceed 0.03 and had tendency to decrease with increasing amount of magnesium content due to the replacement of magnesium ions into barium ion or so-called A-site substitution which could reduce the dielectric constant, tetragonality and especially, the loss tangent.

Table 4.4 Dielectric properties of magnesium-doped barium strontium titanate, $Ba_{1-x-y}Sr_xMg_yTiO_3$ powder were measured at 10 MHz

$Ba_{1-x-y}Sr_xMg_yTiO_3$		Measured at 10 MHz	
x	y	Dielectric constant	Loss tangent
0.3	0	422.93	0.0171
	0.005	369.12	0.0125
	0.01	337.99	0.0154
	0.02	299.19	0.0129
0.4	0	341.28	0.0155
	0.005	330.17	0.0143
	0.01	324.15	0.0143
	0.02	268.34	0.0120
0.5	0	328.80	0.0160
	0.005	313.00	0.0143
	0.01	292.88	0.0114
	0.02	163.10	0.0106

4.6 Acknowledgements

The author thank the partial scholarship and partial funding of the research work provided by The Petroleum and Petrochemical College, Chulalongkorn University. Department of Materials Engineering, Kasetsart University and Kasetsart University Research and Development Institute (KURDI).

4.7 References

[1] Alexandru, H., Berbecaru, C., Ioachim, A., Toacsen, M., Banciu, M., Nedelcu, L. and Ghetu, D. (2004). Oxides ferroelectric (Ba, Sr) TiO_3 for microwave devices. Materials Science and Engineering: B 109(1), 152-159.

[2] Su, B. and Button, T. (2004). Microstructure and dielectric properties of Mg-doped barium strontium titanate ceramics. Journal of applied physics 95(3), 1382-1385.

[3] Basantakumar Sharma, H., Tandon, R., Mansingh, A. and Rup, R. (1993). Dielectric and piezoelectric properties of sol-gel-derived barium titanate ceramics. Journal of materials science letters 12(22), 1795-1796.

[4] Tian, H.-Y., Luo, W.-G., Pu, X.-H., Qiu, P.-S., He, X.-Y. and Ding, A.-l. (2000). Synthesis and analyses of thermal decomposition and microstructure of Sr-doped barium titanate alkoxide derived precipitates and thin films. Thermochimica Acta 360(1), 57-62.

[5] Somani, V. and Kalita, S.J. (2007). Synthesis and characterization of nanocrystalline Barium Strontium Titanate powder via sol-gel processing. Journal of electroceramics 18(1-2), 57-65.

[6] Wang, J., Zhang, J. and Yao, X. (2010). Dielectric properties of Mg-doped $Ba_{0.6}Sr_{0.4}TiO_3$ ceramics prepared by using sol–gel derived powders. Journal of Alloys and Compounds 505(2), 783-786.

[7] García-Hernández, M., García-Murillo, A., Carrillo-Romo, F.d., Jaramillo-Vigueras, D., Chadeyron, G., De la Rosa, E. and Boyer, D. (2009). Eu-Doped $BaTiO_3$ Powder and Film from Sol-Gel Process with Polyvinylpyrrolidone Additive. International Journal of Molecular Sciences 10(9), 4088-4101.

[8] Xu, S., Qu, Y. and Zhang, C. (2009). Effect of Mg^{2+} content on the dielectric properties of $Ba_{0.65-x}Sr_{0.35}Mg_xTiO_3$ ceramics. Journal of Applied Physics 106(1), 014107.

[9] Nedelcu, L., Ioachim, A., Toacsan, M., Banciu, M.G., Pasuk, I., Berbecaru, C. and Alexandru, H.V. (2011). Synthesis and dielectric characterization of $Ba_{0.6}Sr_{0.4}TiO_3$ ferroelectric ceramics. Thin Solid Films 519(17), 5811-5815.